

1 Open integrated distance sampling for modelling age- 2 structured population dynamics

3 Erlend B. Nilsen^{1,2,*} & Chloé R. Nater¹

4 1: Department for Terrestrial Biodiversity, Norwegian Institute for Nature Research
5 (NINA), 7034 Trondheim, Norway

6 2: Faculty of Biosciences and Aquaculture (FBA), Nord University, 7713 Steinkjer, Norway

7 * correspondence: erlend.nilsen@nina.no

8 ORCID: EBN: 0000-0002-5119-8331; CRN: 0000-0002-7975-0108

9

10 Abstract

11 *Estimation of abundance and demographic rates for populations of wild species is a*
12 *challenging but fundamental issue for both ecological research and wildlife management. One*
13 *set of approaches that has been used extensively to estimate abundance of wildlife populations*
14 *is Distance Sampling (DS) for line or point transect survey data. The first implementations of*
15 *DS models were only available as closed population models, and did not allow for the*
16 *estimation of changes in abundance through time. The advent of open population*
17 *formulations based on the DS framework greatly extended the scope of the models, but much*
18 *untapped potential remains in models that estimate temporal dynamics not only in abundance*
19 *but also in the underlying demographic rates. Here, we present an integrated distance*
20 *sampling approach that utilizes age-structured survey data and auxiliary data from marked*
21 *individuals to jointly estimate population density and the demographic rates (recruitment*
22 *rate and survival probability) that drive temporal changes in density. The resulting model is*
23 *equivalent to an integrated population model with a two age classes: juveniles and adults. The*
24 *integrated framework allows making full use of the available data by effectively combining*
25 *line transect and telemetry data, and can easily be adapted to include additional and/or*
26 *different data types. Moreover, as demographic rates often respond to environmental*
27 *variation, our approach also supports direct estimation of the effects of such environmental*
28 *covariates on demographic rates. Through a comprehensive simulation study we show that*
29 *the model is able to adequately recover true population and vital rate dynamics. Subsequent*
30 *application to data from a study of willow ptarmigan (*Lagopus lagopus*) in Norway showcases*
31 *the frameworks ability to recover both fluctuations and trends in population dynamics and*
32 *highlights its potential applicability to a wide range of species surveyed using distance*
33 *sampling approaches.*

34

35 1. Introduction

36 Estimating abundance and demographic rates for wildlife populations is an integral part of
37 basic and applied ecology (Skalski, Ryding, and Millspaugh 2005; Williams, Nichols, and
38 Conroy 2002). Over the last few decades, tremendous progress has been made towards this
39 end. This progress is partly driven by development and application of new field data
40 collection methods and approaches, such as citizen science data (Danielsen et al. 2022),
41 camera trap data (Hamel et al. 2013) and the collection of environmental DNA data (Beng
42 and Corlett 2022). In addition, developments of novel statistical methods alongside
43 decreases in computational costs now allow researchers to estimate abundance and
44 demographic rates in situations where it was not feasible before (Zipkin et al. 2021).
45 Combined, these advances put us in a much better position for estimating quantities needed
46 for population management (Williams, Nichols, and Conroy 2002) and indices relevant for
47 large scale policy applications, e.g. Essential Biodiversity Variables (Kissling et al. 2018).

48 Until recently, joint estimation of population dynamics and demography has relied mostly
49 on data from marked individuals and associated open-population capture-mark-recapture
50 models (Schaub and Kéry 2021). While such methods can provide valuable information for
51 both ecological research and management, collecting the necessary data is typically costly
52 and logistically challenging to implement over large areas. Monitoring programmes
53 focusing on abundance trends over larger areas, on the other hand, are typically based on
54 data from unmarked animals. One often used approach for such surveys is distance
55 sampling (DS). DS has been used for estimating animal abundance in a wide range of
56 contexts and for a variety of taxa (Buckland et al. 2015). One reason for the method's
57 popularity is that it requires neither marking of individuals nor repeated visits to the same
58 sites for estimating detection probability. This makes DS particularly useful for
59 implementation in participatory monitoring programs, allowing stakeholders to take part in
60 the data collection process.

61 Classical implementations of DS models have used closed-population formulations,
62 i.e. models that treat estimates of population density or abundance at different time points
63 as independent and do not including an explicit formulation of the process model that links
64 abundance across years based on estimates of population growth rate (λ) or underlying
65 demographic rates (Buckland et al. 2015). In recent years, DS approaches have been
66 extended in many ways, including applications that estimate changes in abundance over
67 time in open populations via a hidden state model representing population dynamics
68 (Moore and Barlow 2011; Sollmann et al. 2015; Schaub and Kéry 2021). This has greatly
69 extended the potential of DS approaches for studying ecological dynamics across time and
70 space. However, while these latter frameworks may allow to accurately quantify population
71 changes, they typically provide little information on the drivers of these changes, i.e. the
72 underlying vital rates. In fact, if the data does not contain information about the age (and/or
73 sex-) structure of the surveyed population, there is no straightforward way to estimate
74 demographic rates from such data. On the contrary, if age (and sex) of detected individuals
75 can be determined, this information can be used to provide information on recruitment
76 rates and survival probabilities. Nilsen and Strand (2018), for example, used a model based
77 on harvest statistics and observations of population age structure to estimate population

78 abundance and demographic rates without the need for any additional data from marked
79 individuals.

80 Concurrent with the development of more sophisticated DS models, another group of
81 models has emerged and rapidly gained popularity, not least for their ability to disentangle
82 demographic processes underlying population dynamic: integrated population models
83 (IPMs, Schaub and Kéry 2021). Through joint analysis of multiple datasets (or multiple
84 components of the same dataset), IPMs allow simultaneous estimation of population size
85 and composition, as well as all vital rates that form part of an underlying age- or stage-
86 structured population model. Since both DS models and IPMs estimate population
87 size/density, a combination of the two frameworks has the potential to provide good
88 estimates of both population- and demographic parameters by maximizing knowledge
89 gained from transect surveys by augmenting them with other available data (e.g. Schmidt
90 and Robison 2020).

91 In this study, we present a new integrated distance sampling model (IDSM) which
92 integrates data from line transect distance sampling survey data and survival data from
93 marked animals. The model's core is a stage-structured matrix population model that
94 projects population size from one time step to the next based on underlying survival and
95 recruitment rates. We first present the model and assess its robustness and performance
96 through applications to simulated data. By doing so, we showcase how distance sampling
97 models can be used to not only estimate population density but also demographic rates in
98 an IPM setting. Finally, we proceed to highlight the potential of this new modelling
99 framework by applying it to a case study involving data collected on willow ptarmigan
100 (*Lagopus lagopus*) in Central Norway.

101

102 2. Methods

103 2.1 Integrated distance sampling model

104 Our open population integrated distance sampling model (IDSM) consists of two major
105 components: a latent structured population model and a set of likelihoods for data
106 originating from distance sampling surveys and auxiliary survival monitoring of marked
107 birds. In the example case, these auxiliary data come from a radio-telemetry study, but in
108 principle other types of capture-recapture data can also be used.

109 2.1.1 Age-structured population model

110 The population model follows a post-breeding census and includes two age classes:
111 juveniles (young of the year) and adults (> 1 year of age, [Figure 1](#)). This structure
112 commonly used for populations of passerine and game birds (Williams, Nichols, and Conroy
113 2002; Schaub and Kéry 2021). In the context of our willow ptarmigan case study (see
114 below), the population census is set in late summer - which is when the annual distance-
115 sampling survey takes place. At this time, the juvenile class is about 1 - 2 months old.

116 Both juveniles and adults survive from year t census to year $t + 1$ census with survival
117 probability S_t . We assume that individuals can reproduce already as 1-year olds, meaning
118 all survivors may produce offspring in late June which recruit into the population as
119 juveniles just prior to the census in year $t + 1$ according to a recruitment rate R_{t+1} . The
120 changes in densities of juveniles and adults in the population, D_{juv} and D_{ad} , can thus be
121 expressed as

$$122 \begin{aligned} D_{juv,t+1} &= D_{ad,t+1} * R_{t+1} \\ D_{ad,t+1} &= S_t * (D_{juv,t} + D_{ad,t}) \end{aligned}$$

123 or, alternatively, in matrix notation as

$$124 \begin{bmatrix} D_{juv,t+1} \\ D_{ad,t+1} \end{bmatrix} = \begin{bmatrix} S_t * R_{t+1} & S_t * R_{t+1} \\ S_t & S_t \end{bmatrix} \begin{bmatrix} D_{juv,t} \\ D_{ad,t} \end{bmatrix}$$

125 Note that recruitment rate R is defined as juveniles/adult (not juveniles/female). We
126 assume no stochasticity beyond time-variation in vital rates in the model for population
127 density itself, but instead treat local population sizes (numbers of birds in age class a in
128 year t within the area of each transect j , $N_{a,j,t}$), as outcomes of a Poisson process with an
129 expected average equaling $D_{a,t}$ times the transect area (see below). We also make the
130 simplifying assumption that there is no age- or sex-dependence of vital rates, but this
131 assumption could be relaxed by including additional auxiliary data (Israelsen et al. 2020;
132 Sandercock et al. 2011).

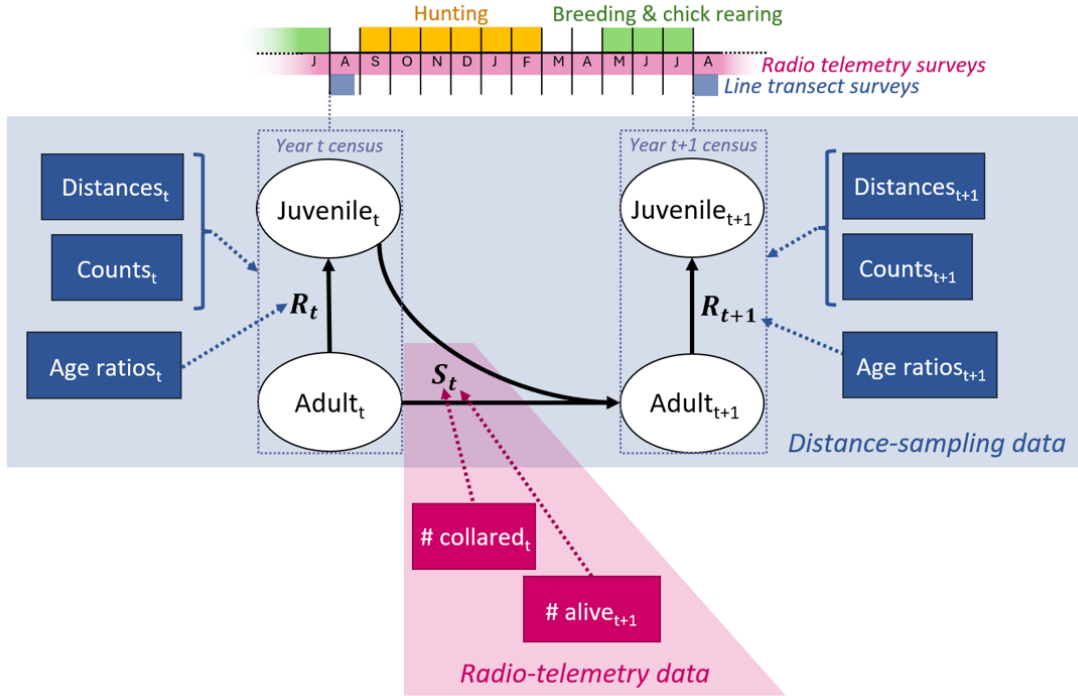


Figure 1: Graphical representation of the annual ptarmigan life cycle with two age classes under a post-breeding census and the data sources included in the integrated distance sampling model. Solid arrows represent relationships within the ptarmigan life cycle; dotted arrows visualize information flow from data sources to parameters. Blue and pink data nodes originate from distance sampling and line transect surveys, respectively. $Juvenile_t$ = juveniles in year t . $Adult_t$ = adults in year t . R_t = recruitment rate in year t . S_t = survival probability from year t to $t + 1$.

133 2.1.2 Likelihoods for distance sampling data

134 The implementation of the modelling framework we present assumes that the distance
 135 sampling survey data have the following characteristics: 1) the survey consists of line
 136 transects, 2) animals may be detected alone or in groups, and 3) juveniles and adults can be
 137 distinguished during surveys. These characteristics are inspired by our willow ptarmigan
 138 case study (details below). Our model includes three likelihoods for different components
 139 of the age-structured distance sampling data. First is the likelihood for the perpendicular
 140 detection distances from line transect, y , which are linked to distance-dependent detection
 141 probability p_y through a half-normal detection function:

$$142 \quad p_y = \exp\left(-\frac{y^2}{2\sigma^2}\right)$$

143 where σ is the half-normal detection parameter. We assumed σ to vary among years (index
 144 t) but not between transect lines or animal group sizes. Following Moore and Barlow
 145 (2011), the resulting σ_t can be used to calculate effective strip width (esw_t) and,

146 consequently, average detection probability per line transect with a truncation distance W
 147 according to:

$$148 \quad esw_t = \sqrt{\frac{\pi * \sigma_t^2}{2}}$$

$$\hat{p}_t = esw_t / W$$

149 The estimated average detection probability \hat{p}_t is an integral part of the second data
 150 likelihood which relates the observed number of animals in each age class a , $obsN_{a,j,t}$ ($j =$
 151 transect) to the corresponding true number per transect, $N_{a,j,t}$:

$$152 \quad obsN_{a,j,t} \sim Poisson(\hat{p}_t * N_{a,j,t})$$

153 $N_{juv,j,t}$ and $N_{ad,j,t}$ are then linked back to the population model by converting them to
 154 densities through multiplication by $2L_{j,t}W$ (where $L_{j,t}$ is length of transect j in year t , and
 155 W is the truncation distance).

156 The third data likelihood focuses on the counts of adults ($obsAd_{j,t}$) and juveniles ($obsJuv_{j,t}$)
 157 observed during the distance sampling surveys and links them to the estimated year-
 158 specific recruitment rate:

$$159 \quad obsJuv_{j,t} \sim Poisson(\widehat{R}_t * obsAd_{j,t})$$

160 *2.1.3 Likelihood for radio-telemetry data*

161 The final likelihood is for the auxiliary telemetry data. It is set up under the assumption of
 162 perfect detection, and hence known fates, of animals bearing transmitters and links the
 163 numbers of animals released at the start of season k of year t to the number of survivors at
 164 the end of the same season:

$$165 \quad survivors_{k,t} \sim Binomial(released_{k,t}, \widehat{Sk}_t)$$

166 Here, Sk_t is the survival probability over the relevant time interval k in year t . The length
 167 and definition of k will be specific to any given study. For the remainder of this article, we
 168 define k as 6-month seasons to be consistent with our ptarmigan case study. Consequently,
 169 the annual survival probability, S_t that appears in the population model above is calculated
 170 as the product of two seasonal survival probabilities, $S1_t$ and $S2_t$.

171 *2.1.3 Hierarchical models with time-variation in parameters*

172 Vital rates (survival probabilities S_t , recruitment rates R_t) and detection parameters (half-
 173 normal detection parameters σ_t) can all be modelled as time-dependent in our framework.
 174 For both the tests with simulated data and the case study described below, we implemented
 175 log-normally distributed random year effects on recruitment rate and detection probability.
 176 In the case study, we additionally included a covariate effect (see details below) on log
 177 recruitment rates, resulting in the following model:

$$178 \quad \log(R_t) = \log(\mu_R) + \beta * cov_t + \epsilon_t$$

179 μ_R represents the mean recruitment rate if the covariate cov_t is centered around 0 (e.g. z-
180 standardized) or a baseline recruitment rate corresponding to $cov_t = 0$ if the covariate is
181 not centered. β the slope of the covariate effect, and ϵ_t the normally distributed random
182 effects.

183 In both simulations and the case study, we treated survival as time-invariant. This was
184 motivated by our case study: previous research has relatively low interannual variation in
185 survival of our focal ptarmigan population (Israelsen et al. 2020) and the telemetry data
186 used in this study has limited potential for accurately estimating time-variation as it is
187 relatively sparse. We note, however, that also survival could be modelled as time-
188 dependent if sufficient data is available.

189 2.2 Model testing with simulated data

190 We assessed the model's overall performance and ability to estimate abundance,
191 demographic rates, and detection parameters without bias by testing it on simulated data.
192 We generated a total of 10 simulated datasets in five steps. First, we simulated 15-year
193 time-series of survival and recruitment rates from biologically plausible values for averages
194 and – in the case of recruitment – among-year variation in demographic rates (survival was
195 held constant across years). Second, we used the yearly demographic rate and realistic
196 initial population densities to simulate stochastic population dynamics in 50 distinct sites.
197 Third, we simulated the grouping of individuals in each site by first determining the
198 expected number of groups in a site (based on the average group size of 5.6 from our
199 ptarmigan data) and then distributing individuals among groups via multinomial trials.
200 Fourth, we assigned a distance from transect line to each group and simulated the line
201 transect survey in all 50 sites across 15 years. Finally, we simulated 5-year time-series of
202 radio-telemetry data (= survival from one year to the next) for a subset of individuals (30
203 per year on average) using the simulated survival probabilities for each relevant year. We
204 then fit the IDSM to each of the 10 simulated datasets three times, using distinct seeds for
205 both simulating initial values and initiating and running the MCMC. Model implementation
206 for simulated data tests was largely identical to that for real data and is described in detail
207 below. For assessing model performance, fit, and bias, we 1) compared model estimates to
208 the true values of parameters used for data simulations visually, 2) correlated estimated
209 and true values, and 3) calculated two metrics to measure bias: the proportion of samples
210 above the true value (corresponding to Bayesian p-values) and the root-mean square
211 deviation (RMSD).

212 2.3 Case study

213 To demonstrate the applicability of the IDSM to real data, we applied it to a case study of
214 willow ptarmigan, a small grouse species with a has a circumpolar distribution (Fuglei et al.,
215 2020). In Norway, there has been a long-term decline in willow ptarmigan abundance
216 across more than a century (Hjeljord and Loe 2022), but in the last few decades abundance
217 trends have fluctuated substantially both across time and space. Willow ptarmigan is a
218 valued game species (see e.g. Andersen et al. (2014)), and there have been several long-
219 term research projects devoted to understanding how they respond to environmental
220 variation and harvest management (Israelsen et al. 2020; Sandercock et al. 2011). A key

221 insight from across several study areas is the the annual recruitment rate (i.e. R_t in our
222 model, as outlined above) is highly variable, and is affected both by spring conditions
223 (Eriksen et al. 2023) and the abundance of small rodents, which constitute alternative prey
224 for common predators (i.e. the Alternative Prey Hypothesis; see Hagen (1952); Kausrud et
225 al. (2008); Bowler et al. (2020)). Adult survival show less inter-annual fluctuations
226 (Israelsen et al. 2020), although variation due to e.g. harvest management is evident when
227 comparing across studies (Israelsen et al. 2020; Sandercock et al. 2011).

228 Our case study was based on an ongoing long-term research project on willow ptarmigan in
229 Lierne municipality in Central Norway (approximately 62.4 degrees north and 13.2 degrees
230 east). The study area is located in a sub-alpine ecosystem, and the landscape is a mosaic of
231 open heath and shrub vegetation (dominated by Ericacea, willow shrub *Salix spp.*, and
232 dwarf birch *Betula nana*), interspersed with bogs and forest patches (mainly birch *Betula*
233 *spp.*). The climate is strongly seasonal, with snow typically covering the ground from
234 October/November through April/May.

235 From this study system, two datasets were used for the case study:

- 236 1. Data from a line transect survey program targeting willow ptarmigan operated
237 under the natural resources management authorities (2007-2021, ongoing)
- 238 2. Data from an individual-based monitoring programme based on radio collared
239 willow ptarmigan (2015-2021, ongoing)

240 Line transect survey data were collected in August each year, prior to the annual autumn
241 harvest season, as part of the program “Hønsefuglportalen”. Hønsefuglportalen is a national
242 program for line transect surveys of tetraonid birds, and the effort is directed mainly
243 towards willow ptarmigan habitats. In our case study, we used data from the western part
244 of Lierne municipality. Line transects are surveyed by trained volunteers that use pointing
245 dogs to locate the birds. When located, the geographical coordinate, perpendicular distance
246 from the sampling line, the number of birds in the group, as well as the age (juvenile or
247 adult) and sex of the birds are recorded. As the surveys are conducted in early August,
248 juveniles can be distinguished from adults by their smaller body size. Males and females are
249 mainly distinguished by sound (males often make a characteristic sound when being
250 flushed). Observers are trained to distinguish age classes and sexes, but incomplete
251 identification can occur. In this application we assumed that the resulting “unknown” age
252 and/or sex class birds were in fact juveniles (see discussion for further considerations).
253 Besides bird observations, field workers also record whether (1) or not (0) they encounter
254 small rodents on any transect line, allowing the proportion of transect lines with small
255 rodent detection to be used as measure of rodent occupancy (covariate ranging from 0 to
256 1). After data are collected they undergo quality control, get standardized based on the
257 Darwin-Core standard (Wieczorek 2012), and made publicly available as a sampling-event
258 data set published through GBIF (Nilsen et al. 2023). For additional description of the data
259 collection procedures, see (Bowler et al. 2020; Kvasnes, Pedersen, and Nilsen 2018; Nilsen
260 et al. 2023).

261 The radio-telemetry data is the result of an individual-based longitudinal study over the
262 period 2015-2021. Each winter (in February-March), willow ptarmigan were located at

263 night using snowmobiles and large hand nets with prolonged handles, as described in
264 (Israelsen et al. 2020). High-powered head lamps were used to dazzle the birds and allow
265 capture. Captured birds were fitted with a uniquely numbered leg ring (~ 2.4g) and a
266 Holohil RI-2BM or Holohil RI-2DM radio transmitter (~ 14.1g) and subsequently released.
267 The radio transmitters had an expected battery lifetime of 24 months (RI-2BM) or 30
268 months (RI-2DM), and included a mortality circuit that was activated if a bird had been
269 immobile for 12 hours. We monitored the birds throughout most of the year by
270 triangulation from the ground at least once a month for 10 months of the year (February –
271 November) by qualified field personnel. A number of birds dispersed out of the main study
272 areas and was thus out of signal range for field personnel on the ground. To avoid loss of
273 data, we conducted aerial triangulation using a helicopter or airplane three times a year
274 (May, September and November) in the years 2016-2020. In the analysis here, we assume
275 that the telemetry data is representative for the entire duration of study period (2007-
276 2021), despite its collection only starting in 2015.

277 **2.4 Bayesian model implementation**

278 We implemented the model in a Bayesian framework using NIMBLE version 1.0.1 (Valpine
279 et al. 2017) in R version 4.3.1 (R Core Team 2023). The likelihood for line transect
280 observation distances was set up using a custom half-normal distribution developed by
281 Michael Scroggie as part of the “nimbleDistance” package
282 (<https://github.com/scrogster/nimbleDistance>). We used non-informative uniform priors
283 (with biologically reasonable boundaries where possible) for all parameters. We assumed
284 constant survival and time-varying recruitment rate in models fit to both simulated and real
285 data.

286 For the model fits to simulated and real data we ran 3 (simulated) or 4 (real) MCMC chains
287 with NIMBLE’s standard samples for 100k iterations. 40k thereof were discarded as burn-in
288 prior to thinning with factor 20, leaving us with 3k posterior samples per chain (total of 12k
289 samples per run). MCMC parameters were chosen to yield a representative number of
290 samples from converged chains, and convergence was determined based on visual
291 inspection of trace plots. Posterior samples from the model fitted to real data are available
292 at Nilsen and Nater (2024) (in folder PosteriorSamples_LierneCaseStudy).

293

294 3. Results

295 3.1 Model performance on simulated datasets

296 Models fit to simulated datasets reached MCMC convergence within the given number of
297 iterations. Chain mixing was good for all parameters except average recruitment rate (μ_R);
298 for this parameter, an elevated degree of autocorrelation was visible in the MCMC chains in
299 some of the replicate runs, but models still produced posterior distributions that well
300 represented the true value used in simulations (Figure 2).

301 Posterior estimates relative to true values, Bayesian p-values, and RMSD for parameters
302 estimated in three model fits to each of 10 simulated data sets are shown in Figure 2 and
303 Figure 3. Overall, the IDSM was able to correctly estimate the majority of parameters from
304 all 10 simulated datasets without substantial systematic bias. The replicate runs for each
305 dataset resulted in very similar posterior distributions, demonstrating that the models
306 converged towards the same posterior distributions irrespective of starting values. This
307 may not seem to be the case for survival parameters (Figure 2), but this is largely due to the
308 relatively low number of individuals in the simulated telemetry data; estimated posteriors
309 match up well with simulated numbers of survivors in each datasets, and the averages of
310 Bayesian p-values fell very close to 0.5 (= no bias). For time-variation in recruitment rate
311 (σ_R), on the other hand, the average Bayesian p-value indicated a potential for
312 overestimation ($p = 0.6966667$), and this is consistent with the relatively large spread of
313 Bayesian p-values for year-specific recruitment rates (Figure 3). Across all years, the
314 correlation between predicted and true recruitment rates was very high (slope = 0.981), yet
315 closer inspection showed that slight over- and under-estimation was present for certain
316 years across all replicates (see supplementary figures in folder SimCheck_byDataSet in
317 Nilsen and Nater (2024)). This was also the case for year-specific estimates of population
318 density and detection probability, but both were slightly more likely to be underestimated
319 than overestimated (Figure 3).

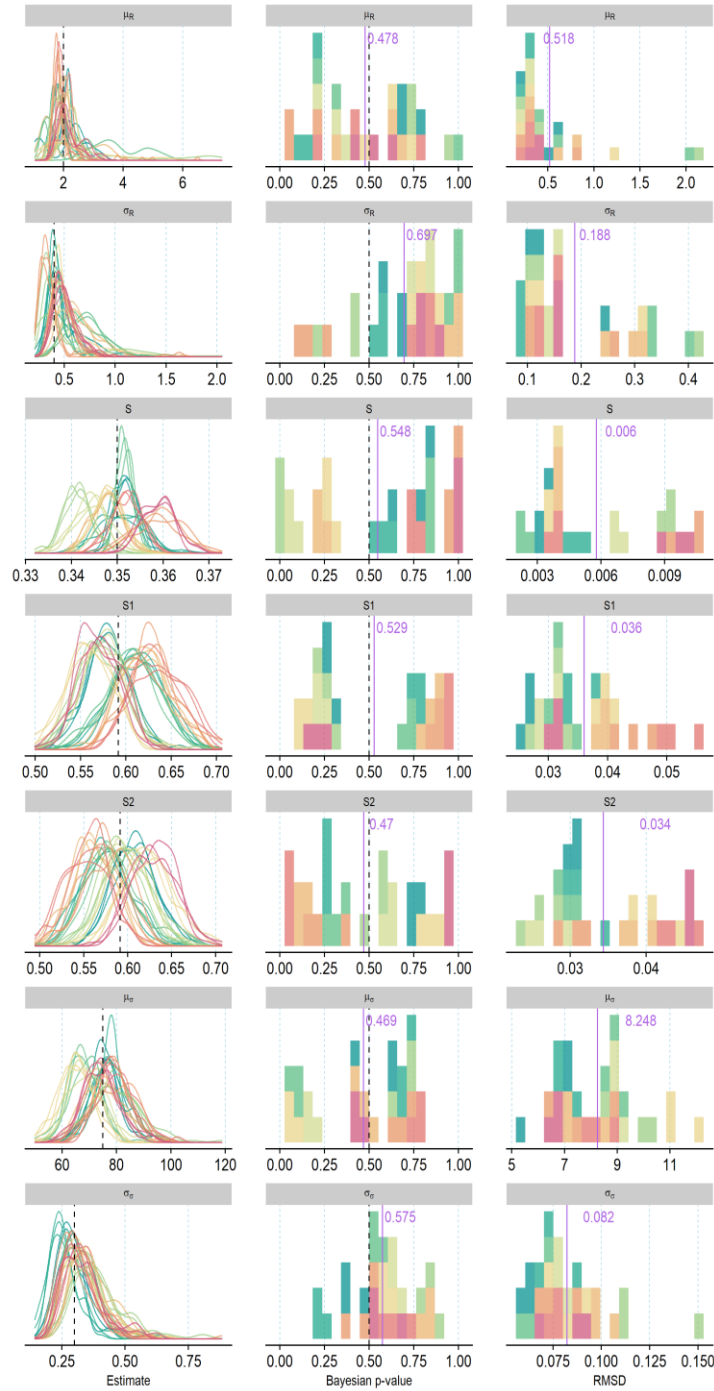


Figure 2: Vital rate and detection parameter averages estimated from 10 distinct sets of simulated data (= colors) using three model fits each. First row depicts posterior densities from each model run relative to the true value used to simulate data (black dashed line). Second and third rows visualize the distributions of Bayesian p-values (proportion of samples $>$ true value) and root-mean square deviations (RMSD) for all model runs, respectively. Purple lines and numbers mark the mean values across all model runs; dashed black line (second row only) marks the ideal Bayesian p-value of 0.5.

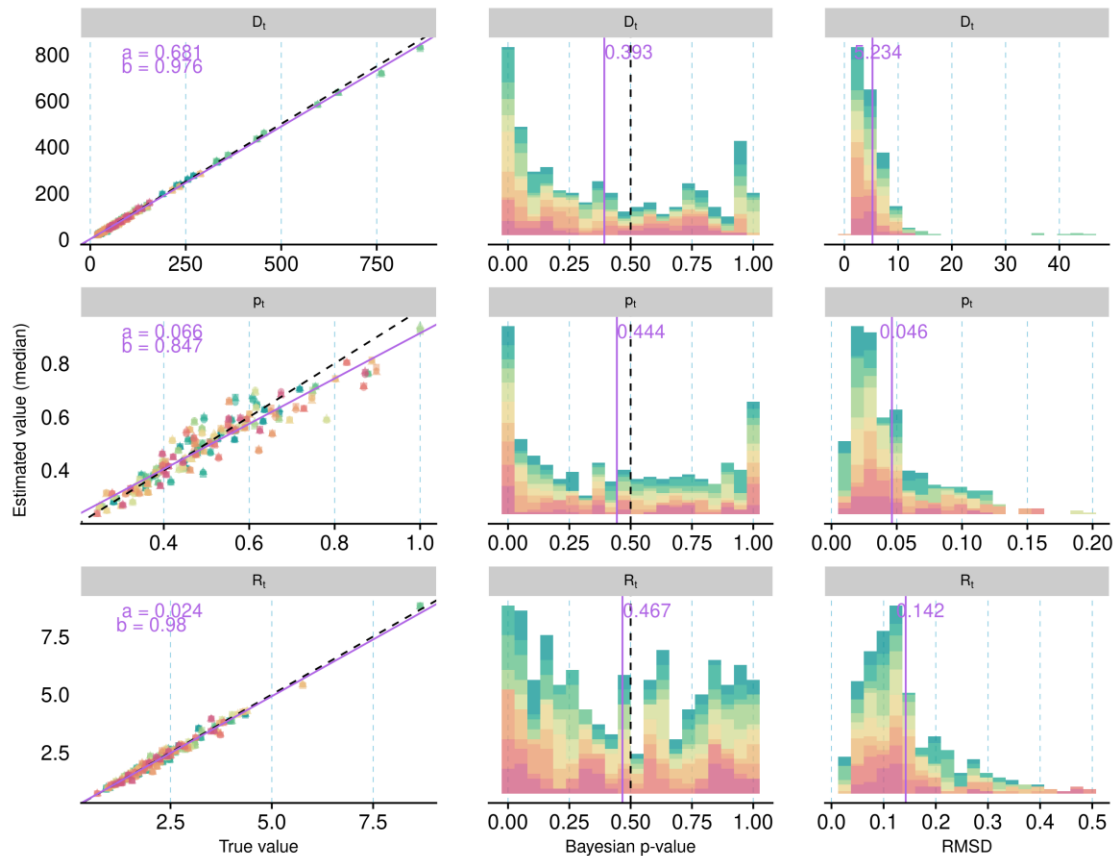


Figure 3: Annual population density (D_t), detection probability (p_t), and recruitment rate (R_t) estimated from 10 distinct sets of simulated data (= colors) using three model fits each. First row depicts the relationship between posterior medians from each model run and the true value used to simulate data (purple solid line = relationship estimated from linear model with a = intercept and b = slope; black dashed line = perfect correlation). Second and third rows visualize the distributions of Bayesian p -values (proportion of samples > true value) and root-mean square deviations (RMSD) for all model runs, respectively. Purple lines and numbers mark the mean values across all model runs; dashed black line (second row only) marks the ideal Bayesian p -value of 0.5. And equivalent figure showing posterior samples instead of posterior means is available in the supplementary material on OSF.

321 3.2 Case study on willow ptarmigans in Central Norway

322 Having evaluated the overall performance of our model on simulated data, we used data
 323 from our case study in Lierne to estimate abundance, vital rates and detection probabilities
 324 from a real-world data set. Like the model fits to simulated data, convergence was reached
 325 within the five amount of iterations and mixing was good, albeit with somewhat higher
 326 chain autocorrelation for the intercept in the recruitment model. Ptarmigan population
 327 density was estimated with a marked increase across the study period, from < 10 ptarmigan

328 / km^2 in 2007 to > 35 ptarmigan / km^2 in 2021 (Figure 4). The increase was most
329 distinct from 2016 and onward.

330 The average probability of detecting individuals and groups of ptarmigan within transect
331 line areas was 0.61 (95% C.I = 0.57 - 0.65), and estimated with a detection decay parameter
332 σ of 95.3 (95% C.I = 82.18 - 110.43). Detection probabilities were highest in the start of the
333 study and in the period 2016-2019 and lowest from 2010-2012. The relationship between
334 detection probability and distance and changes in detection over time are visualized in
335 supplementary figures “DetectionProb_distance.png” and “TimeSeries_pDetect.png” in
336 Nilsen and Nater (2024).

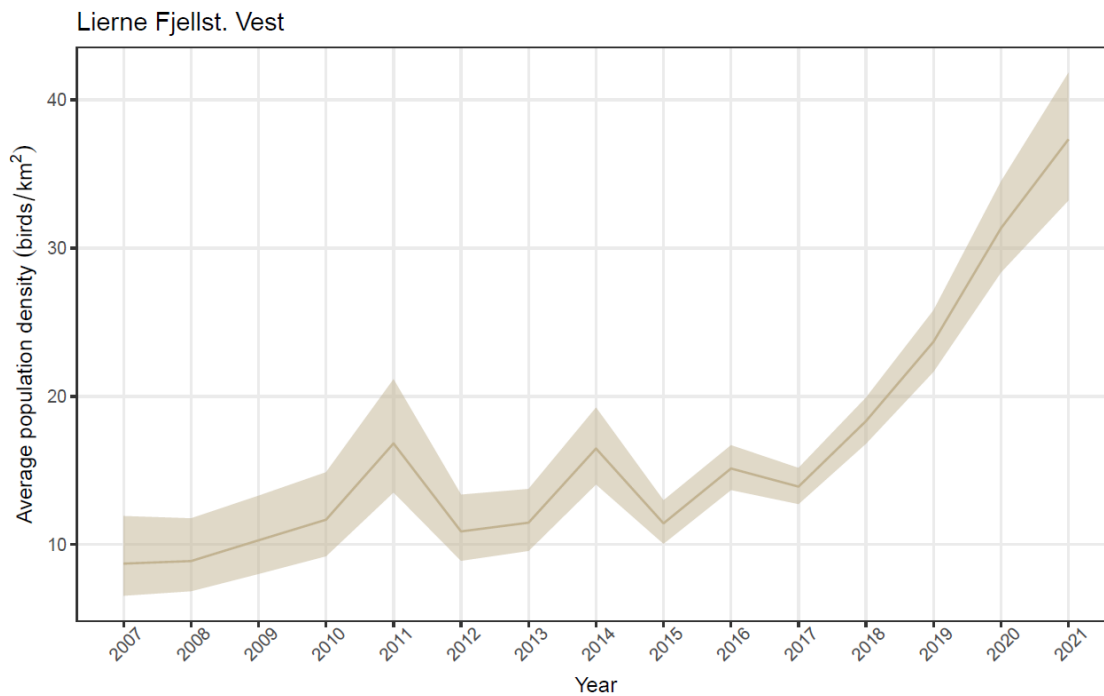


Figure 4: Estimated density of willow ptarmigans in Lierne from 2007 to 2021. Solid line represents the posterior median, ribbon marks 95% credible interval.

337 Average survival probability for August - January (S_1) was estimated at 0.46 (95% C.I = 0.42
338 - 0.5) while average survival probability for February - July (S_2) was estimated as 0.64
339 (95% C.I = 0.59 - 0.7) (Figure 5 A). Annual survival probability S , given by the product of S_1
340 and S_2 , was estimated at 0.3 (95% C.I = 0.29 - 0.31), Figure 5 A).

341 Recruitment (R_t) was allowed to vary across years (see model specification), and estimates
342 displayed large inter-annual variability (Figure 5 C, Figure S1). While the mean (baseline)
343 recruitment μ_R was estimated as 2.7 (95% C.I = 2.3 - 3.2) the yearly recruitment rates
344 ranged from 1.2 in year 2012 to 4.9 in year 2007.

345 Given the available data, the IDSM was not able to estimate a clear effect of small rodent
346 abundance on ptarmigan recruitment (slope-parameter for the z-standardized rodent
347 occurrence data = 0.062 ; 95% C.I. = -0.2 - 0.31, see supplementary figure “Rep_betaR.R.png”
348 in Nilsen and Nater (2024)).

Lierne Fjellst. Vest

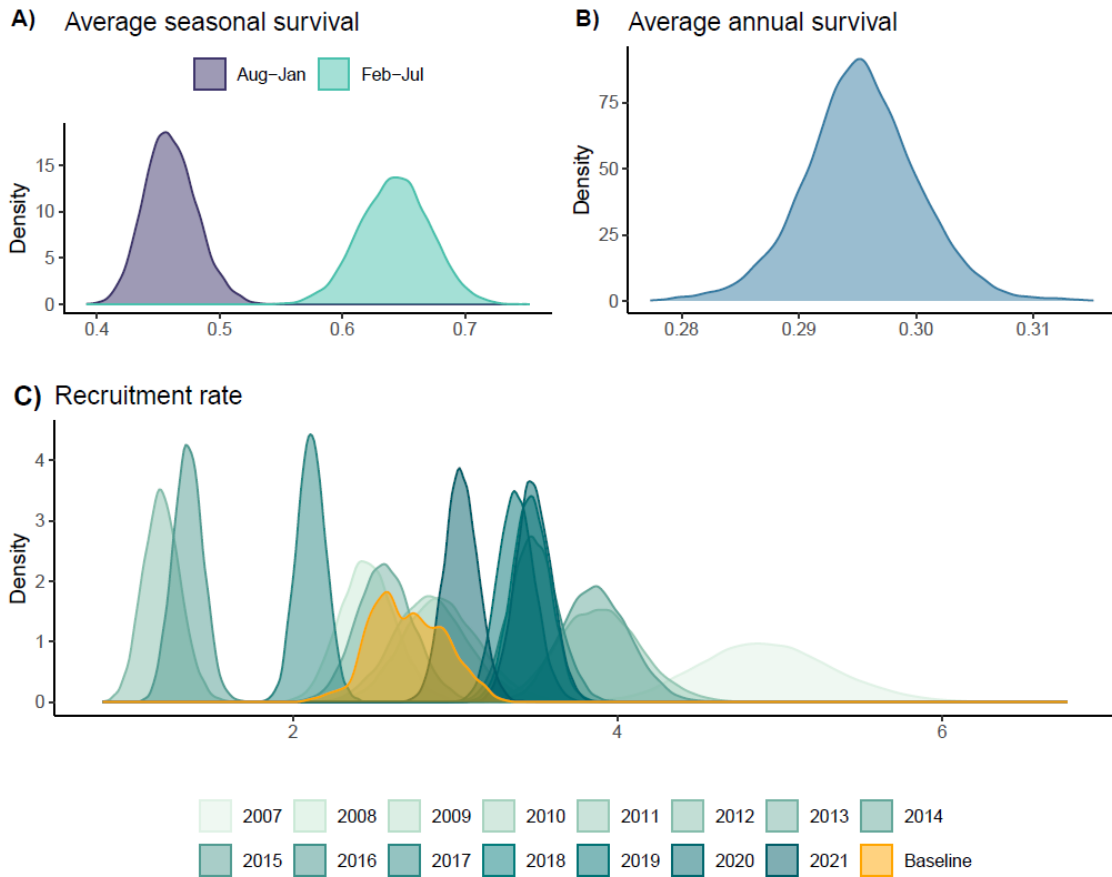


Figure 5: Posterior densities of A) seasonal survival, B) average annual survival, and C) recruitment rate. For the latter, the yellow distribution is for the intercept, representing a baseline recruitment rate when rodent occupancy is low. The turquoise distributions are for year-specific estimates or recruitment rate, with darker colors indicating later years. For a visualization of the time-series of recruitment rates, see supplementary figure "TimeSeries_rRep" on OSF.

349

350

351 4. Discussion

352 We developed an integrated population model that jointly analyses line transect distance
353 sampling survey data and data from marked individuals to estimate population abundance,
354 survival probabilities, and recruitment rates over time. We first used simulated data to
355 examine the model's ability to recover the underlying parameters when they were known.
356 We then fitted the model to data from an ongoing field study on willow ptarmigan in
357 Norway to showcase its applicability to real wildlife monitoring data.

358 Open population formulations of the distance sampling model have previously been
359 presented and applied to various ecological systems (Sollmann et al. 2015; Bowler et al.
360 2020; Moore and Barlow 2011). The model presented here extends those previous
361 applications by formulating the underlying population process model as a stage-structured
362 matrix model (Caswell 2000) in which the matrix elements are represented by annual
363 survival probabilities and recruitment rates. While this has been the common approach for
364 a range of other statistical modelling frameworks, including the growing suite of models
365 falling into the category of integrated population models (Schaub and Kéry 2021), the
366 integration of mechanistic population models into distance sampling frameworks is rather
367 new. The resulting modelling framework allow us to make maximum use of distance
368 sampling data in combination with auxiliary information both from the distance sampling
369 survey itself (i.e. information on age, sex, etc. of observed animals) and from other types of
370 monitoring, and enables estimation not only of changes in population density but also of
371 underlying vital rates over time.

372 In general, the model did a good job at recreating the underlying parameters when fitted to
373 simulated data with known underlying true parameter values. The simulated data sets were
374 based relatively wide ranges of parameter values, yet model posteriors included the true
375 values in almost all cases. While there seems to be potential for overestimating time
376 variation in recruitment rates, this bias did not propagate into estimates of year-specific
377 recruitment rates (Figure 3), and may be related to the subpar mixing of the intercept of the
378 recruitment model. The model was more likely to under- than overestimate detection
379 probabilities and population densities, but bias in these estimates was generally small and
380 spread out across time-series, i.e. bias did not seem to arise disproportionately at e.g. the
381 starts or ends of time-series. Simulated data tests also revealed that telemetry data
382 simulated with an average of 30 individuals may be too sparse to obtain robust and
383 generalisable estimates of seasonal survival probabilities. This could be investigated further
384 by repeating simulated data runs with different average numbers of individuals in the
385 telemetry data, but we chose not to go down this path here as we were primarily interested
386 in model performance given the amounts of data that are currently available for our
387 ptarmigan case study. Based on the simulated data tests presented here, we conclude that
388 the IDSM is able to provide meaningful and sufficiently accurate and robust estimates of
389 demographic parameters from age-structured distance sampling data, provided that the
390 input data are unbiased (with respect to the underlying model formulation).

391 Real data, however, are likely to be subject to certain biases, which may result in biased
392 parameter estimates unless accounted for. One type of bias that is likely to be common for
393 age-structured distance sampling data arises from failure to (correctly) classify the age

394 class of observed individuals. In our case study on willow ptarmigan in Norway, such
395 misclassification is likely to happen at an unknown rate, even if the size difference between
396 adult and juvenile birds are quite substantial during the survey. Moreover, The probability
397 for misclassification might be related to both the timing of the survey (e.g. mid August
398 rather than early August), it might vary between observers, and even by survey conditions.
399 Observations with incorrectly classified age have the potential to introduce bias in the
400 IDSMs relative estimates of survival and recruitment. This is due to the way it uses the
401 distance sampling data to estimate survival and recruitment rates. In our process model,
402 the population growth rate (λ) is determined by the survival and recruitment rate in the
403 following way: $\lambda = S + (S * R)$, and this creates a dependence between the demographic
404 parameters. If the age ratio in the data are biased or contain frequent misclassifications, this
405 is likely to affect the relative contribution of survival and recruitment to the growth rate. To
406 get an idea of the potential effect of this on parameter estimation, we checked the
407 sensitivity of the output of the model fit to real data with regard to the treatment of birds
408 classified as “unknown sex and age” by the field personnel (see Methods). In the model
409 version presented in the results section, we made the assumption that these birds were in
410 fact juveniles. Comparing estimates to an alternative scenario in which we discarded all
411 birds classified as “unknown sex and age” (see supplementary figures in Nilsen and Nater
412 (2024)) we found that – as expected – estimated population density was virtually
413 unaffected by the treatment of “unknown sex and age” observations, while the annual
414 demographic parameters shifted proportional to the amount of “unknown sex and age”
415 observations in the given year (towards higher recruitment and lower survival). Thus,
416 biases in the reported age ratios may affect estimated of demographic rates, but not so
417 much population density. Since the proportion of “unknown sex and age” observations in
418 our ptarmigan case study was low (< 3% of observations), potential biases in estimates
419 resulting from age misclassification are expected to be small. Nonetheless, future
420 developments of the IDSM modelling framework should focus on ways of accounting
421 explicitly for misclassification of age class in the field.

422 The density estimates that we derived from the case study on Willow ptarmigan in Norway
423 is comparable to previous estimates from across Norway (see e.g. Sandercock et al. (2011);
424 Kvasnes, Pedersen, Solvang, et al. (2014)). Throughout the study period from 2007 - 2021,
425 the density increased markedly, but the reason for this increase is not known. Compared to
426 previous studies on ptarmigan (see e.g. (Israelsen et al. 2020; Sandercock et al. 2011)), we
427 could have expected somewhat higher estimates of survival probability. One potential
428 reason for the overall lower estimates obtained here is that our IDSM analysis assumed
429 constant survival over the period 2007-2021 while survival, in reality, may have changed
430 over time. If survival in more recent years, when telemetry data was collected (and the
431 study of e.g. Israelsen et al. (2020) was carried out) was higher than in earlier years –
432 something that seems likely given population increase over recent years – an average over
433 the entire time period is expected to be lower. On a different note, we can also not exclude
434 the possibility of a small degree of bias in survival estimates due to misclassification of age
435 in the data (see above), especially seeing as the IDSM’s recruitment rate estimates also
436 appear somewhat high compared to other studies on willow ptarmigan (Eriksen et al. 2023;
437 Kvasnes, Pedersen, Storaas, et al. 2014; Steen et al. 1988). As the ptarmigan case study
438 served as an illustrative example for the IDSM framework in this article, we did not further

439 investigate alternative models, such as implementations with time-varying survival or
440 different treatment of uncertainty in age and/or sex. The model lends itself easily to such
441 extensions, however, and methods such as posterior predictive checks and WAIC will be
442 useful for assessing and optimizing the fit of the model to data from relevant case studies
443 (Hooten and Hobbs 2015; Conn et al. 2018).

444 In addition to estimating demographic rates from line transect data, the IDSM also allows
445 including relevant environmental effects on the demographic rates themselves, and not just
446 on population growth rate as a whole (λ). In the ptarmigan case study we thus attempted to
447 investigate the effect of small rodent abundance (approximated as the proportion of
448 transect lines on which rodents were reported each year) on recruitment rate. We were not
449 able to detect a clear effect of rodent abundance due to large uncertainty associated with
450 the estimate (see Supplementary Figures “Rep_betaR.R.png” in Nilsen and Nater (2024)).
451 This may seem somewhat surprising given that such a pattern has been reported
452 repeatedly in the literature (see e.g. Bowler et al. (2020)). We speculate that there are at
453 least three potential and not mutually exclusive explanations to this result. The first is that
454 our covariate data may not have been well suited for estimating effects on recruitment. The
455 data on rodent abundance was heavily zero-inflated, and the annual variation in the index
456 was rather small otherwise, making for a covariate with relatively little information
457 content. While this may be partially a consequence of how these data are collected, it is also
458 well known that the amplitude and regularity of the rodent cycles has been fading in recent
459 decades (Kausrud et al. 2008; Cornulier et al. 2013), and our study area might be no
460 exception. Lack of peak rodent years in the time series to which we fitted the model may
461 thus also have contributed to making effect estimation challenging. Second, it is possible
462 that rodent effects were obscured by other, potentially stronger, covariate effects. Previous
463 research has shown that ptarmigan recruitment is also sensitive to the weather in the late
464 winter and spring (before and during the breeding season); as we did not fit any weather
465 covariates to the model, there is a possibility that effects of spring conditions in certain
466 years may have masked any remaining effects of small rodent abundance. Finally, the data
467 set used in this analysis is relatively short (15 years), leaving us with somewhat limited
468 statistical power to detect effects of temporal covariates. Taken together we therefore do
469 not consider this study as a particularly strong test of the underlying effect of small rodent
470 fluctuations on ptarmigan recruitment rates. It is worth noting that future applications
471 could increase statistical power by including either more years of data or capitalizing on
472 space-for-time substitution as the Norwegian ptarmigan monitoring programme spans
473 many more locations beyond Lierne. Bowler et al. (2020), for example, used data from the
474 same sampling program but from more areas using a simpler open population DS model,
475 and detected a very clear signal from small rodent abundance on ptarmigan population
476 growth rate. An extension of our IDSM to include data from multiple areas therefore
477 constitutes a promising approach for investigating to which extent similar results emerge
478 by linking environmental covariates to the actual demographic rates and not only just to the
479 resulting population growth rates.

480 The new IDSM framework presented here is relevant for many wildlife populations that are
481 surveyed using line transect sampling that includes additional information on age, sex,
482 and/or life stages of the observed individuals. Following the integrated modelling

483 philosophy, the IDSM also allows for the integration of auxiliary data. In our application
484 here, we integrated data from radio-telemetry of marked birds, which explicitly supported
485 the estimation of survival probabilities. The IDSM framework is very flexible, however, and
486 open to the inclusion of additional/other auxiliary data that contains information on
487 demographic rates or population size/density. Moreover, the hierarchical nature of the
488 model makes it straightforward to adapt to different species and to include different suites
489 of environmental covariates on the demographic rates. Finally, it constitutes a modelling
490 framework that is well suited for extension to multiple areas and thus able to capitalize on
491 space-for-time substitution (Lovell et al. 2023) to produce large-scale and spatially explicit
492 estimates of population density, demographic rates, and environmental effects from large-
493 scale (participatory) monitoring.

494 **Author contributions**

495 **Erlend B. Nilsen:** Conceptualization, Methodology, Software, Formal analysis, Investigation,
496 Data Curation, Writing - Original Draft, Writing - Review & Editing, Project administration,
497 Funding acquisition.

498 **Chloé R. Nater:** Conceptualization, Methodology, Software, Validation, Formal analysis,
499 Investigation, Data Curation, Writing - Original Draft, Writing - Review & Editing,
500 Visualization.

501 **Acknowledgements**

502 We are grateful to field workers that collected the line transect data through the
503 Hønsfuglportalen program. Fjellstyrene i Lierne and many colleagues from NINA and Nord
504 University contributed both to the line transect program and the field work related to the
505 marked willow ptarmigan. We also thank James A. Martin for constructive discussions
506 during the later stages of this work and Simon Hansul, Tiago Marquez, and Sandrine Charles
507 for constructive feedback on the manuscript during the review process.

508 **Funding**

509 Both data collection and analytical work were financed by the Norwegian Environment
510 Agency funded the projects (grant nrs 17010522, 19047014 and 22047004).

511 **Conflict of interest disclosure**

512 The authors declare that they comply with the PCI rule of having no financial conflicts of
513 interest in relation to the content of the article

514 **Data and code availability**

515 The raw data from the line transect surveys is deposited on GBIF and can be accessed freely
516 via the Living Norway Data Portal (<https://data.livingnorway.no>). The work here is based
517 on version 1.7 of the dataset "Tetraonid line transect surveys from Norway: Data from
518 Fjellstyrene" (Nilsen et al. 2023).

519 The auxiliary radio-telemetry data and rodent occupancy data, all code used for wrangling,
520 analysing, and visualizing data and results, as well as vignettes providing rich text
521 documentation of all steps in the workflows for simulated and real data analysis, can be
522 found in the project's repository on GitHub:
523 https://github.com/ErlendNilsen/OpenPop_Integrated_DistSamp. The results presented in
524 this paper were created using version 1.5 of the code (Nater et al. 2024).

525 Supplementary figures and posterior samples from the model run on the real data are
526 available as a time-stamped open archived on Open Science Framework (Nilsen and Nater
527 2024).

528

529 **References**

530 Andersen, O., B. P. Kaltenborn, J. Vitterso, and T. Willebrand. 2014. "Preferred Harvest
531 Principles and - Regulations Amongst Willow Ptarmigan Hunters in Norway." *Wildlife*
532 *Biology* 20 (5): 285–90. <https://doi.org/10.2981/wlb.00048>.

533 Beng, K. C., and R. T. Corlett. 2022. "Applications of Environmental DNA (eDNA) in Ecology
534 and Conservation: Opportunities, Challenges and Prospects." *Biodiversity and Conservation*
535 29: 2089–2121. <https://doi.org/10.1007/s10531-020-01980-0>.

536 Bowler, D. E., M. A. J. Kvasnes, H. C. Pedersen, B. K. Sandercock, and E. B. Nilsen. 2020.
537 "Impacts of Predator-Mediated Interactions Along a Climatic Gradient on the Population
538 Dynamics of an Alpine Bird." *Proceedings of the Royal Society - Series B* 287 (1941):
539 20202653. <https://doi.org/10.1098/rspb.2020.2653>.

540 Buckland, Stephen T, Eric A Rexstad, Tiago André Marques, Cornelia Sabrina Oedekoven, et
541 al. 2015. *Distance Sampling: Methods and Applications*. Vol. 431. Springer.

542 Caswell, Hal. 2000. *Matrix Population Models*. Vol. 1. Sinauer Sunderland, MA.

543 Conn, Paul B, Devin S Johnson, Perry J Williams, Sharon R Melin, and Mevin B Hooten. 2018.
544 "A Guide to Bayesian Model Checking for Ecologists." *Ecological Monographs* 88 (4): 526–
545 42.

546 Cornulier, Thomas, Nigel G. Yoccoz, Vincent Bretagnolle, Jon E. Brommer, Alain Butet,
547 Frauke Ecke, David A. Elston, et al. 2013. "Europe-Wide Dampening of Population Cycles in
548 Keystone Herbivores." *Science* 340 (6128): 63–66.
549 <https://doi.org/10.1126/science.1228992>.

550 Danielsen, Finn, Hajo Eicken, Mikkel Funder, Noor Johnson, Olivia Lee, Ida Theilade,
551 Dimitrios Argyriou, and Neil D. Burgess. 2022. "Community Monitoring of Natural Resource
552 Systems and the Environment." *Annual Review of Environment and Resources* 47 (1): 637–
553 70. <https://doi.org/10.1146/annurev-enviro-012220-022325>.

554 Eriksen, Lasse Frost, Thor Harald Ringsby, Hans Chr. Pedersen, and Erlend B. Nilsen. 2023.
555 "Climatic Forcing and Individual Heterogeneity in a Resident Mountain Bird: Legacy Data

- 556 Reveal Effects on Reproductive Strategies." *Royal Society Open Science* 10 (5): 221427.
557 <https://doi.org/doi:10.1098/rsos.221427>.
- 558 Hagen, Yngvar. 1952. *Rovfuglene Og Viltpleien*. Gyldendal Norsk forlag.
- 559 Hamel, S., S. T. Killengreen, J. A. Henden, N. E. Eide, L. Roed-Eriksen, R. A. Ims, and N. G.
560 Yoccoz. 2013. "Towards Good Practice Guidance in Using Camera-Traps in Ecology:
561 Influence of Sampling Design on Validity of Ecological Inferences." *Methods in Ecology and*
562 *Evolution* 4 (2): 105–13. [https://doi.org/DOI 10.1111/j.2041-210x.2012.00262.x](https://doi.org/DOI%2010.1111/j.2041-210x.2012.00262.x).
- 563 Hjeljord, Olav, and Leif Egil Loe. 2022. "The Roles of Climate and Alternative Prey in
564 Explaining 142 Years of Declining Willow Ptarmigan Hunting Yield." *Wildlife Biology* 2022
565 (6): e01058. <https://doi.org/https://doi.org/10.1002/wlb3.01058>.
- 566 Hooten, Mevin B, and N Thompson Hobbs. 2015. "A Guide to Bayesian Model Selection for
567 Ecologists." *Ecological Monographs* 85 (1): 3–28.
- 568 Israelsen, Markus F, Lasse F Eriksen, Pål F Moa, Bjørn Roar Hagen, and Erlend B Nilsen.
569 2020. "Survival and Cause-Specific Mortality of Harvested Willow Ptarmigan (*Lagopus*
570 *Lagopus*) in Central Norway." *Ecology and Evolution* 10 (20): 11144–54.
571 <https://doi.org/10.1002/ece3.6754>.
- 572 Kausrud, K. L., A. Mysterud, H. Steen, J. O. Vik, E. Ostbye, B. Cazelles, E. Framstad, et al. 2008.
573 "Linking Climate Change to Lemming Cycles." *Nature* 456 (7218): 93–U3.
574 <https://doi.org/10.1038/nature07442>.
- 575 Kissling, W. Daniel, Jorge A. Ahumada, Anne Bowser, Miguel Fernandez, Néstor Fernández,
576 Enrique Alonso García, Robert P. Guralnick, et al. 2018. "Building Essential Biodiversity
577 Variables (EBVs) of Species Distribution and Abundance at a Global Scale." *Biological*
578 *Reviews* 93 (1): 600–625. <https://doi.org/10.1111/brv.12359>.
- 579 Kvasnes, M. A. J., H. C. Pedersen, and E. B. Nilsen. 2018. "Quantifying Suitable Late Summer
580 Brood Habitats for Willow Ptarmigan in Norway." *BMC Ecology* 18 (1): 41.
581 <https://doi.org/10.1186/s12898-018-0196-6>.
- 582 Kvasnes, M. A. J., H. C. Pedersen, T. Storaas, and E. B. Nilsen. 2014. "Large-Scale Climate
583 Variability and Rodent Abundance Modulates Recruitment Rates in Willow Ptarmigan
584 (*Lagopus Lagopus*)." *Journal of Ornithology* 155 (4): 891–903.
585 <https://doi.org/10.1007/s10336-014-1072-6>.
- 586 Kvasnes, M. A. J., Hans Chr. Pedersen, H. Solvang, T. Storaas, and Erlend B. Nilsen. 2014.
587 "Spatial Distribution and Settlement Strategies in Willow Ptarmigan." *Population Ecology* 57
588 (1): 151–61. <https://doi.org/10.1007/s10144-014-0454-1>.
- 589 Lovell, Rebecca SL, Sinead Collins, Simon H Martin, Alex L Pigot, and Albert B Phillimore.
590 2023. "Space-for-Time Substitutions in Climate Change Ecology and Evolution." *Biological*
591 *Reviews* 98 (6): 2243–70. <https://doi.org/10.1111/brv.13004>.

- 592 Moore, Jeffrey E, and Jay Barlow. 2011. "Bayesian State-Space Model of Fin Whale
593 Abundance Trends from a 1991-2008 Time Series of Line-Transect Surveys in the California
594 Current." *Journal of Applied Ecology* 48 (5): 1195–205. [https://doi.org/10.1111/j.1365-
595 2664.2011.02018.x](https://doi.org/10.1111/j.1365-2664.2011.02018.x).
- 596 Nater, C. R., ErlendNilsen, christofferhohi, M. Grainger, and B. B. Niebuhr. 2024.
597 "ErlendNilsen/OpenPop_Integrated_DistSamp: Ptarmigan IDSM v1.5." Zenodo.
598 <https://doi.org/10.5281/zenodo.13627743>.
- 599 Nilsen, E. B., and C. R. Nater. 2024. "Supplementary Information to "an Integrated Open
600 Population Distance Sampling Approach for Modelling Age-Structured Populations."
601 Archive. <https://doi.org/10.17605/OSF.IO/TPRV2>.
- 602 Nilsen, E. B., and O. Strand. 2018. "Integrating Data from Multiple Sources for Insights into
603 Demographic Processes: Simulation Studies and Proof of Concept for Hierarchical Change-
604 in-Ratio Models." *PLoS One* 13 (3): e0194566.
605 <https://doi.org/10.1371/journal.pone.0194566>.
- 606 Nilsen, E. B., R. Vang, M. Kjønsgberg, and M. A. J. Kvasnes. 2023. "Tetraonid Line Transect
607 Surveys from Norway: Data from Fjellstyrene." Dataset. <https://doi.org/10.15468/975ski>.
- 608 R Core Team. 2023. *R: A Language and Environment for Statistical Computing*. Vienna,
609 Austria: R Foundation for Statistical Computing. <https://www.R-project.org/>.
- 610 Sandercock, Brett, Erlend B Nilsen, Henrik Brøseth, and Hans Chr Pedersen. 2011. "Is
611 Hunting Mortality Additive or Compensatory to Natural Mortality? Effects of Experimental
612 Harvest on the Survival and Cause-Specific Mortality of Willow Ptarmigan." *Journal of
613 Animal Ecology* 80 (1): 244–58. <https://doi.org/10.1111/j.1365-2656.2010.01769.x>.
- 614 Schaub, Michael, and Marc Kéry. 2021. *Integrated Population Models: Theory and Ecological
615 Applications with r and JAGS*. Academic Press.
- 616 Schmidt, Joshua H, and Hillary L Robison. 2020. "Using Distance Sampling-Based Integrated
617 Population Models to Identify Key Demographic Parameters." *Journal of Wildlife
618 Management* 84 (2): 372–81. <https://doi.org/10.1002/jwmg.21805>.
- 619 Skalski, John, Kristin Ryding, and Joshua Millspaugh. 2005. *Wildlife Demography: Analysis of
620 Sex, Age, and Count Data*. Academic Press.
- 621 Sollmann, Rahel, Beth Gardner, Richard B Chandler, J Andrew Royle, and T Scott Sillett.
622 2015. "An Open-Population Hierarchical Distance Sampling Model." *Ecology* 96 (2): 325–31.
623 <https://doi.org/10.1890/14-1625.1>.
- 624 Steen, J. B., H. Steen, N. C. Stenseth, S. Myrberget, and V. Marcström. 1988. "Microtine
625 Density and Weather as Predictors of Chick Production in Willow Ptarmigan, *Lagopus
626 Lagopus*." *Oikos* 51 (3): 367–73. <https://doi.org/10.2307/3565320>.
- 627 Valpine, Perry de, Daniel Turek, Christopher J Paciorek, Clifford Anderson-Bergman,
628 Duncan Temple Lang, and Rastislav Bodik. 2017. "Programming with Models: Writing

- 629 Statistical Algorithms for General Model Structures with NIMBLE.” *Journal of Computational*
630 *and Graphical Statistics* 26 (2): 403–13. <https://doi.org/10.1080/10618600.2016.1172487>.
- 631 Wieczorek, David AND Guralnick, John AND Bloom. 2012. “Darwin Core: An Evolving
632 Community-Developed Biodiversity Data Standard.” *PLOS ONE* 7: 1–8.
633 <https://doi.org/10.1371/journal.pone.0029715>.
- 634 Williams, Byron K, James D Nichols, and Michael J Conroy. 2002. *Analysis and Management*
635 *of Animal Populations*. Academic press.
- 636 Zipkin, Elise F, Erin R Zylstra, Alexander D Wright, Sarah P Saunders, Andrew O Finley,
637 Michael C Dietze, Malcolm S Itter, and Morgan W Tingley. 2021. “Addressing Data
638 Integration Challenges to Link Ecological Processes Across Scales.” *Frontiers in Ecology and*
639 *the Environment* 19 (1): 30–38. <https://doi.org/https://doi.org/10.1002/fee.2290>.